INTERNATIONAL JOURNAL OF CLIMATOLOGY
Int. J. Climatol. (2009)
Published online in Wiley InterScience
(www.interscience.wiley.com) DOI: 10.1002/joc.1893

RMetS
Royal Meteorological Society

A climatology of warm-season mesoscale convective complexes in subtropical South America

Joshua D. Durkee[a]* and Thomas L. Mote[b]

[a] *Meteorology Program, Department of Geography and Geology, Western Kentucky University, Bowling Green, KY, USA*
[b] *Climatology Research Laboratory, Department of Geography, University of Georgia, Athens, GA, USA*

ABSTRACT: This study extends investigations of mesoscale convective complexes (MCCs) over subtropical South America (SSA) by describing the physical characteristics of MCCs during the austral warm season (October–May) for 1998–2007 in SSA. Within the nine warm seasons, 330 events were documented. An average of 37 MCCs occurred each warm season and reached a maximum cloud-shield size of 256 500 km^2, and lasted 14 h on average. Although 85% of the MCC population occurred over the South American continent, the remaining systems that occurred over the adjacent Atlantic Ocean were significantly larger by nearly 30%. These findings show MCCs in SSA are larger and longer-lived than shown in previous work. Compared to the United States, MCCs in SSA are significantly larger with longer durations. Unlike the US systems, these events do not exhibit much poleward migration throughout the warm season. The highest frequency and concentration of MCC cloud shields are centred east of the Andes Mountains between 20 °S and 30 °S over Paraguay, northern Argentina, and southern Brazil throughout the warm season. As a result, relationships between latitude, and MCC maximum extent or duration are weak or non-existent, respectively. There is, however, a moderate positive relationship between duration and maximum extent. Ultimately, MCCs in SSA are large, long-lasting events that possess great potential for contributing significantly to precipitation totals across the region. Copyright © 2009 Royal Meteorological Society

KEY WORDS mesoscale convective complex; South America; climatology

Received 21 March 2008; Revised 6 February 2009; Accepted 14 February 2009

1. Introduction

Subtropical South America (SSA) is a region susceptible to frequent heavy precipitation events. This region – southern Bolivia, southern Brazil, Paraguay, northern Argentina, and Uruguay – is home to the world's fifth largest river basin, the La Plata Basin (Figure 1). The La Plata Basin comprises 30% of the Earth's fresh water supply and drains one quarter of the entire continent. As one of world's top food producers, the economy of the region largely thrives from livestock and crop harvests. The Paraná, Paraguay, and Uruguay Rivers help supply nearly 80% of the basin's electricity through hydropower technologies. Moreover, the world's largest hydroelectric power plant facility is located along the Paraná River at the Itaipú Dam on the Brazil/Paraguay border. Overall, the La Plata Basin generates 70% of the combined Gross National Product of the countries within the basin (Mechoso *et al*., 2001).

Indeed, one of the greatest threats for SSA is frequent occurrences from some of the world's most intense thunderstorm complexes [e.g. mesoscale convective systems (MCSs)] and their resultant heavy precipitation (Salio *et al*., 2007; Vera *et al*., 2006; Zipser *et al*., 2006; Silva and Berbery, 2006; Nieto Ferreira *et al*., 2003; Carvalho *et al*., 2002; Velasco and Fritsch, 1987, among others). MCSs are comprised of individual thunderstorms organized together as a larger-scale weather system with a contiguous precipitation area. Heavy rainfall from MCSs is often associated with floods, which can be disastrous to livestock, crops, and humankind. Undoubtedly, the lack of MCS rainfall could also be detrimental to the region's agricultural communities. Therefore, understanding the characteristics and role that MCSs play in the subtropical hydroclimate of South America is imperative.

2. Background

Much attention has been devoted towards understanding interactions between the physical landscapes of South America with certain synoptic and mesoscale processes conducive to MCS development (Salio *et al*., 2007; Zipser *et al*., 2006; Silva and Berbery, 2006; Nieto Ferreira *et al*., 2003; Mota, 2003; Carvalho *et al*., 2002, among others). Results from many of those studies include descriptions of physical characteristics of MCSs. However, the majority of those studies are limited in temporal scope to a few years or less. Even fewer studies of South American thunderstorms have focused on

* Correspondence to: Joshua D. Durkee, Department of Geography and Geology, 1906 College Heights Blvd., Western Kentucky University, Bowling Green, KY 42101, USA. E-mail: joshua.durkee@wku.edu

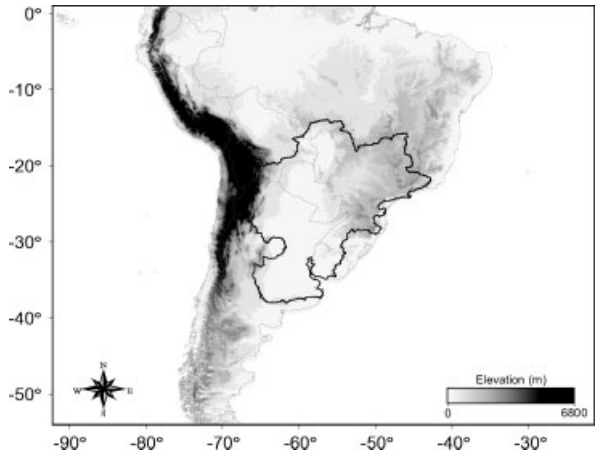

Figure 1. Elevation map of South America. The perimeter of the La Plata Basin is indicated by the bold outline.

mesoscale convective complexes (MCCs) (e.g. Laing and Fritsch, 1997, 2000; Figueiredo and Scolar, 1996; Duquia and Silva Dias, 1994; Rocha, 1992; Scolar and Figueiredo, 1990; Silva Dias *et al*., 1987; Velasco and Fritsch, 1987; Guedes, 1985; Guedes and Silva Dias, 1984). MCCs, the largest MCS sub-class, exhibit large quasi-circular cloud shields (i.e. $\geq$50 000 km^2) that persist for $\geq$6 h (Table I). MCCs have been widely studied in other parts of the world, including Africa (Laing and Fritsch, 1993a; Laing *et al*., 1999), India (Laing and Fritsch, 1993b), China (Miller and Fritsch, 1991), Australia (James, 1992), Europe (Laing and Fritsch, 1997), and most notably North America (Maddox, 1980; Rodgers *et al*., 1983; Merritt and Fritsch, 1984; Kane *et al*., 1987; Tollerud *et al*., 1987; Cotton *et al*., 1989; McAnelly and Cotton, 1989; Tollerud and Rodgers, 1991; Tollerud and Collander, 1993; Anderson and Arritt, 1998; Ashley *et al*., 2003, among others). A summary of global MCC populations and their large-scale environments was developed by Laing and Fritsch (1997, 2000).

Previous MCC research has shown these particular systems are capable of producing tornadoes, severe hail, and damaging winds. However, on the basis of the spatial and temporal thresholds originally set forth by Maddox (1980), heavy precipitation must be regarded as a cause of several of the hazards produced by MCCs (Maddox, 1983; Houze *et al*., 1990). Perhaps the greatest hazards that result from heavy precipitation are persistent regional flooding, localized flash floods, mudslides, and property and crop damage (Maddox, 1979, 1980, 1983; Tollerud *et al*., 1987; McAnelly and Cotton, 1989; Houze *et al*., 1990; Anderson and Arritt, 1998).

In addition, Maddox (1980) found one in five MCCs in the USA led to injuries or deaths, while Rogers *et al*. (1983) found 27 of the 37 reported flash-flood-producing MCCs in the USA during 1982 resulted in numerous injuries and casualties. Anderson and Arritt (1998) indicated that the extensive 1993 Midwestern flood was in part, attributed to 18 of the 27 recorded MCCs that resulted in many reports of injuries, deaths, and property and crop damage. In South America, Velasco and Fritsch (1987) found 11 floods and 13 casualties were attributed to 13 of the 78 MCCs during 1981–1983. Little research has documented MCC hazards outside of the Americas.

Despite the documented negative impacts of MCC rainfall, numerous studies have also suggested that MCC precipitation is vital for sustaining agriculture and farming industries in the Great Plains and Midwest regions of the USA (Fritsch *et al*., 1986; Tollerud and Collander, 1993; Ashley *et al*., 2003). Fritsch *et al*. (1986) suggested that MCC rainfall may help sustain balanced soil moisture budgets and possibly prevent the onset of drought. Ashley *et al*. (2003) and Fritsch *et al*. (1986) showed that MCCs have contributed up to 60% of the total precipitation in portions of the central USA. Laing *et al*. (1999) demonstrated that MCCs contributed an average of 22% of the total rainfall during July–September 1987 across portions of the Sahel in Africa. On the basis of the findings and suggestions from previous studies, it is clear that MCCs possess the potential to have a large impact on precipitation patterns of a region. One such region that has been shown to experience recurring MCC activity similar to the USA is the subtropics of South America.

Compared to the global population of MCCs, North and South American systems share many similarities. Ashley *et al*. (2003) and Laing and Fritsch (2000) found the mean location for MCC genesis and initiation for the Americas are located on the lee side of major mountain ranges (Rockies and Andes) over plain regions. MCCs over both continents also commonly develop within similar atmospheric environments; baroclinic zones that contain high values of low-level vertical wind shear ($\geq$6–8 m s^{-1}) and convective available potential energy (CAPE) ($\geq$1500 J kg^{-1}); areas of maximized warm, moist air transport via a low-level jet; and upper-level divergence superimposed low-level convergence with the advancement of an approaching (and often weak) mid-level short-wave (Maddox, 1980; Laing and Fritsch, 2000). In one of the few available studies that explicitly focuses on the South American MCC population for a study period greater than 1 year, Velasco

Table I. Mesoscale convective complex definition based on analyses of IR satellite imagery.

Mesoscale convective complex (MCC) definition[a]	
Criterion	Physical characteristics
Size	Interior cold–cloud region with temperature of −52 °C must have an area of 50 000 km^2
Initiation	Size definition first satisfied
Duration	Size definition must be met for a period of $\geq$6 h
Maximum extent	Contiguous cold–cloud shield (IR temperature −52 °C) reaches maximum size
Shape	Eccentricity (minor axis/major axis) 0.7 at time of maximum extent
Terminate	Size definition is no longer satisfied

[a] MCC definition originally developed by Maddox (1980).

DOI: 10.1002/joc

and Fritsch (1987) (hereafter, VAF) documented an average of 39 events during November–April across SSA for 1981–1983. The 15-year MCC climatological dataset put forth by Ashley *et al.* (2003) shows an average of 35 events for the USA annually. Both sets of events display similar diurnal patterns whereby MCC initiation generally occurs during the late afternoon/early evening hours, and reach maximum size near midnight, before dissipating during the morning.

Differences in MCC physical characteristics between the two studies show that, while the annual frequency of all events was similar in North and South America, South America had a much higher frequency of larger systems. These South American MCCs also had mean lifecycles up to 2 h longer and average continuous cold cloud-shield areas nearly 23 000 km^2 greater in size. [Note that this difference might be conservative as VAF used an 8°–12 °C colder cloud-shield threshold than the original MCC criteria by Maddox (1980) due to modified IR image enhancement.] VAF and Laing and Fritsch (2000) attribute these physical differences to greater moisture supply from the Amazon Basin, steeper mid-level lapse rates influenced from the upstream Andes, and higher tropopause heights.

The knowledge base for when and where these events occur and the atmospheric environments conducive to their development has been established for North America. However, in order to advance our understanding of South American MCCs, particularly in the subtropics, a climatological database of a longer duration is needed. The possibility remains that the physical traits of the events documented in VAF might be biased given their short period of record (2 years). In fact, VAF note the frequency of events between the 2 years they observed ranges from 22 to 56, the latter occurred during a strong El Niño event. Therefore, a more complete and accurate description of MCCs in SSA may be established with an examination of a longer period of record.

This investigation sets out to address this issue by providing climatological descriptions of the physical characteristics of subtropical South American MCCs during the austral warm season (defined here as October–May) for 1998–2007. High-resolution precipitation products from low-orbiting satellites (e.g. the Tropical Rainfall Measuring Mission) are readily available during 1998–2007 for subsequent studies of MCC rainfall. Results from this study provide a more comprehensive understanding of South American MCCs and the characteristics that underlie these heavy rain producers. This is particularly important for the La Plata Basin, given its dependency on rainfall from events such as MCCs.

3. Data and Methodology

This study adheres to a strictly defined set of MCC cloud-shield criteria observable in infrared (IR) satellite imagery (Table I). Full-disc GOES-8 and GOES-12, 4-km IR satellite data, primarily at three-hourly time intervals, were provided by the National Oceanic Atmospheric Administration Comprehensive Large-array data Stewardship System (National Oceanic Atmospheric Administration (NOAA), 2007 CLASS data available at: http://www.class.ncdc.noaa.gov). The nominal times for the three-hourly satellite images were 0245, 0545, 0845, 1145, 1445, 1745, 2045, and 2345 UTC. There were occasional instances when nominal images were missing, but were available during other times (e.g. 1015 or 0315 UTC).

MCCs were documented using an automated cloud-top identification procedure similar to Augustine (1985). The procedure used here first consists of an automated routine to identify all cloud shields in each satellite image that satisfy the 'size' criterion in Table I. Each group of pixels identified by this criterion was outlined by a polygon to delineate the peripheral border of the cloud shield. In order to determine the orientation and eccentricity of the contoured cloud shield(s), the authors used an empirical orthogonal function (EOF) analysis of pixel coordinates (Jackson, 1991; Carvalho and Jones, 2001). The output for each image time was threefold. First, in one output file each cloud shield was assigned a unique identification based on the year, Julian day, and time of occurrence. Each unique occurrence contains basic output of its physical properties including horizontal area, eccentricity, and longitude/latitude coordinates of the system centroid. Second, the longitude/latitude vertices of the polygon defining the cloud shield were output. The final output was an image of a scene illustrating the contoured outlines of all cloud shields that met MCC 'size' criteria (Figure 2).

The first step for tracking the cloud shields was to manually observe a sequence of scenes. System evolution was handled similar to the Machado *et al.* (1998) approach. When a system was observed to split, the cloud shield that closely resembled the previous scene (often the largest cloud shield within the split) was logged as a continuation of the lifecycle of that system. The remaining cloud shield was documented as

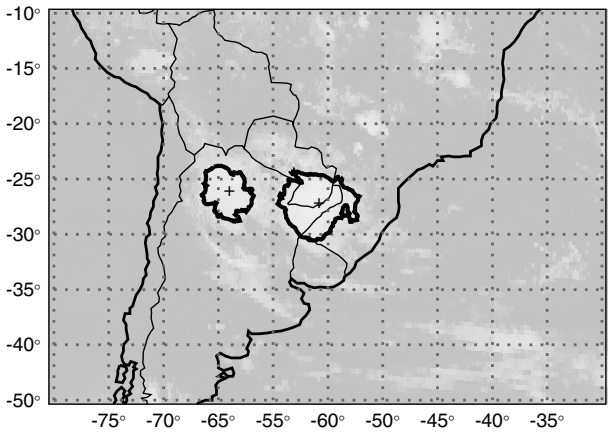

Figure 2. Sample scene from 11 January 2007 illustrating cloud shields that met the MCC 'size' criterion, with the longitude and latitude location of the cloud-shield centroid.

DOI: 10.1002/joc

system initiation and tracked separately as a new event. Merging cloud shields were handled in two ways. If a cloud shield was observed to merge with another smaller system, the lifecycle of the larger system was considered active. In contrast, if a cloud shield was observed to merge with another larger system, the smaller system's lifecycle was considered to terminate at the time of the merge. Manual observation of sequential scenes ensured confidence that the rubrics of splitting and merging systems were handled properly. Once a cloud shield was identified with initiation and termination times that a group of cloud shields was flagged as one event and given a unique system identification. Because the regional focus was on the subtropical region, only systems where any portion of the cloud shield occurred south of 20 °S at any point during its lifecycle were considered. What remained was a catalogue of MCSs for SSA. The final step was to extract only those events which met the 'duration' and 'shape' thresholds in Table I in order to complete the requirements for MCC classification. This process was repeated over October–December and January–May blocks for each warm season spanning 1998–2007.

Other published examples of automated procedures designed to identify mesoscale convection include FORTRACC (Machado *et al*., 1998) and MASCOTTE (Carvalho and Jones, 2001). These procedures are also designed to track and document system lifecycles, thereby eliminating manual observation of successive satellite imagery. Two primary advantages for tracking convective systems using fully automated methods are that the analyses are consistently performed and are time efficient. However, one disadvantage includes the manner in which these routines handle the evolution of a given system (i.e. splitting and merging systems). Machado *et al*. (1998) compared the results between their fully automated method and approaches similar to this study (i.e. hybrid approach). They found that although hybrid approaches tend to handle the propagation trajectories better, the differences between the two methods are minimal for larger datasets. Despite the advantage for one technique over another, the authors of this study believe while the current approach can be somewhat subjective and labour-intensive, it provided an important opportunity to visually determine and verify the splitting or merging of cloud systems.

4. Results

Previous studies provided by Salio *et al*. (2007), Vera *et al*. (2006), Zipser *et al*. (2006), Nieto Ferreira *et al*. (2003), Carvalho *et al*. (2002), and Machado *et al*. (1998) have shown that SSA is highly susceptible to MCS activity. The findings from the current study provide support for the results from VAF that the largest and often longest-lived MCS class, the MCC, is no exception.

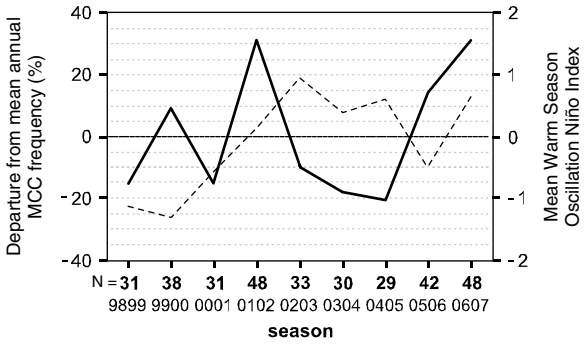

Figure 3. MCC frequency per austral warm-season (October–May) for 1998–2007. Bold line indicates the percent departure from the mean annual average MCC frequency. The dashed line shows the mean Oscillation Niño Index for October–May.

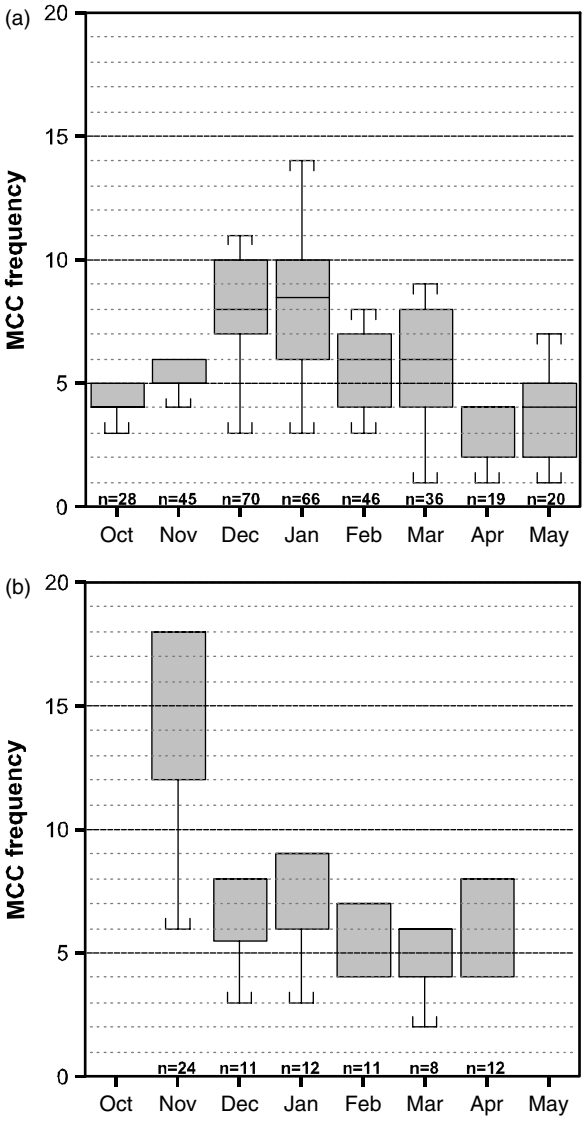

Figure 4. Box and whisker plot of warm-season MCC frequency by month for (a) the years 1998–2007 and (b) 1981–1983 (constructed from data given in Velasco and Fritsch 1987). The boxes show the interquartile range, the whiskers show the 10th and 90th percentiles, and the solid line indicates the median. *N* is equal to the total frequency of events for a given month for the entire period of record.

DOI: 10.1002/joc

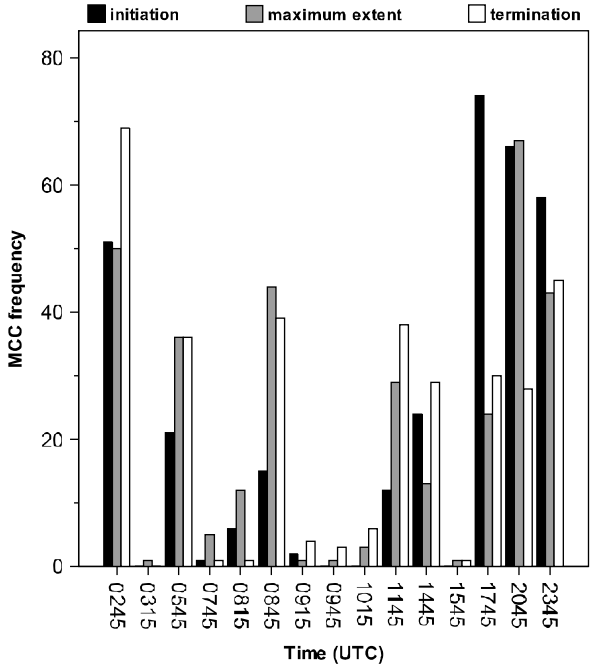

Figure 5. Frequency for all MCCs during storm initiation, maximum size, and termination times.

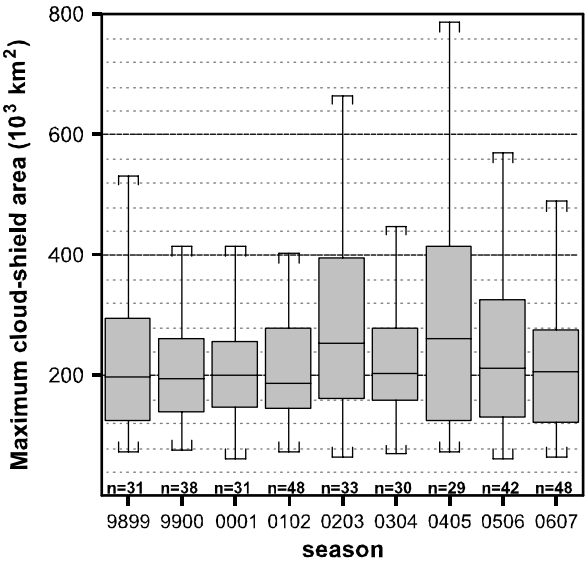

Figure 6. As in Figure 4 except for the maximum cloud-shield size.

4.1. Temporal analysis

For the nine warm seasons during 1998–2007, there were 330 observed MCCs, with a median (average) of 33 (37) events. Figure 3 shows that the signal between anomalous periods of MCC activity and the phase and magnitude of the EI Niño/Southern Oscillation (ENSO) is highly variable. However, in order to accurately describe the interannual variability of MCCs in SSA, as it relates to ENSO, a longer period of record is necessary (Carvalho *et al.* 2002). Given that numerous studies (e.g. Silva and Ambrizzi, 2006; Lau and Zhou, 2003; Grimm *et al.*, 1998, 2000; Ropelewski and Halpert, 1987, 1989; Velasco and Fritsch, 1987) have documented increases in convective activity and precipitation in SSA

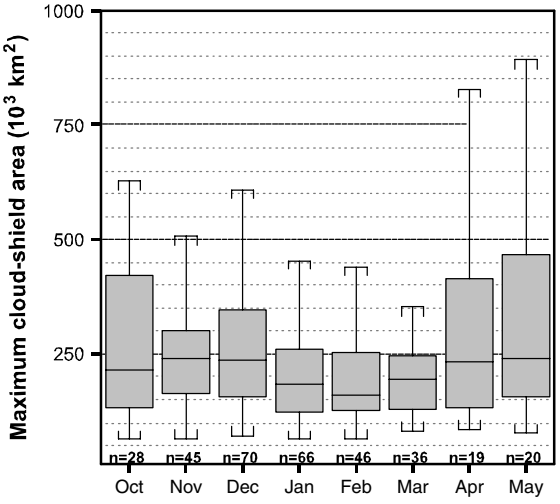

Figure 7. As in Figure 6 except for the monthly.

during El Niño phases, a larger dataset may reveal the possible connection between ENSO and MCC activity. Although mean warm-season frequencies between VAF and this study are similar, there are notable differences in monthly frequencies (*cf* Figure 4(a) and (b)). VAF show November as the month of peak MCC occurrence, while our study shows a peak during December and January. Also, the results of this study show a strong connection between the monthly MCC frequency pattern and the seasonal solar cycle, contrary to the results in VAF.

One disadvantage of analysing 3-hourly satellite images is accurately identifying MCC diurnal patterns and other storm statistics, such as maximum cloud-shield size and system duration. For instance, it is likely that the critical stages outlined in Table I (i.e. storm initiation, when the cloud shield reaches maximum extent, and storm termination) occurred between image times. While this is true regardless of the time interval between images, uncertainty in the interpretation of the diurnal pattern increases with decreasing temporal resolution.

Figure 5 illustrates MCC diurnal frequency for each critical stage. The greatest frequency of occurrence for initiation, maximum extent, and termination occurred between 1745, 2045, and 0245 UTC, respectively. Nearly 75% of all MCCs started between 1745 and 0245 UTC. Meanwhile, 78% reached maximum size between 2045 and 0845 UTC, and 77% dissipated between 2045 and 1145 UTC. Despite the temporal overlap in each stage, MCCs in SSA appear to occur more often at night (between 1745 and 0245 UTC).

The average size of all 330 MCCs at maximum extent was 256 500 km^2 – 27% larger than shown by VAF. The warm-season distribution of maximum cloud-shield sizes shows the 2002–2003 and 2004–2005 seasons had considerably larger MCCs (medians of 252 800 km^2 and 263 400 km^2, respectively), while MCCs in the remaining seasons were closer to 200 000 km^2 (Figure 6). The largest MCCs occurred during late spring to early summer and late fall, while the smallest systems occurred during late summer (Figure 7). The average duration

DOI: 10.1002/joc

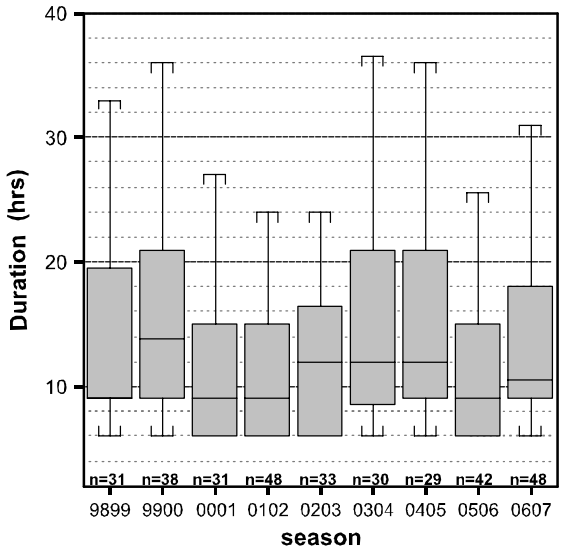

Figure 8. As in Figure 4 except for MCC lifecycle duration.

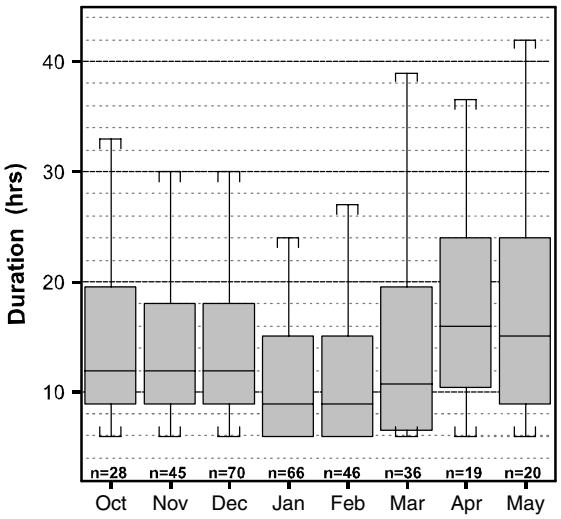

Figure 9. As in Figure 8 except for the monthly.

for all events was 14 h – 2.5 h longer than the duration given by VAF. There is a high degree of variability in MCC duration from year to year (Figure 8). However, it appears that longer-lived storms tend to occur during spring to early summer and fall (Figure 9).

4.2. Spatial analysis

From the nine warm seasons examined in this study, it is clear that MCCs in SSA are particularly large, long-lasting, and relatively frequent events. This section illustrates the spatial distribution of MCCs in SSA.

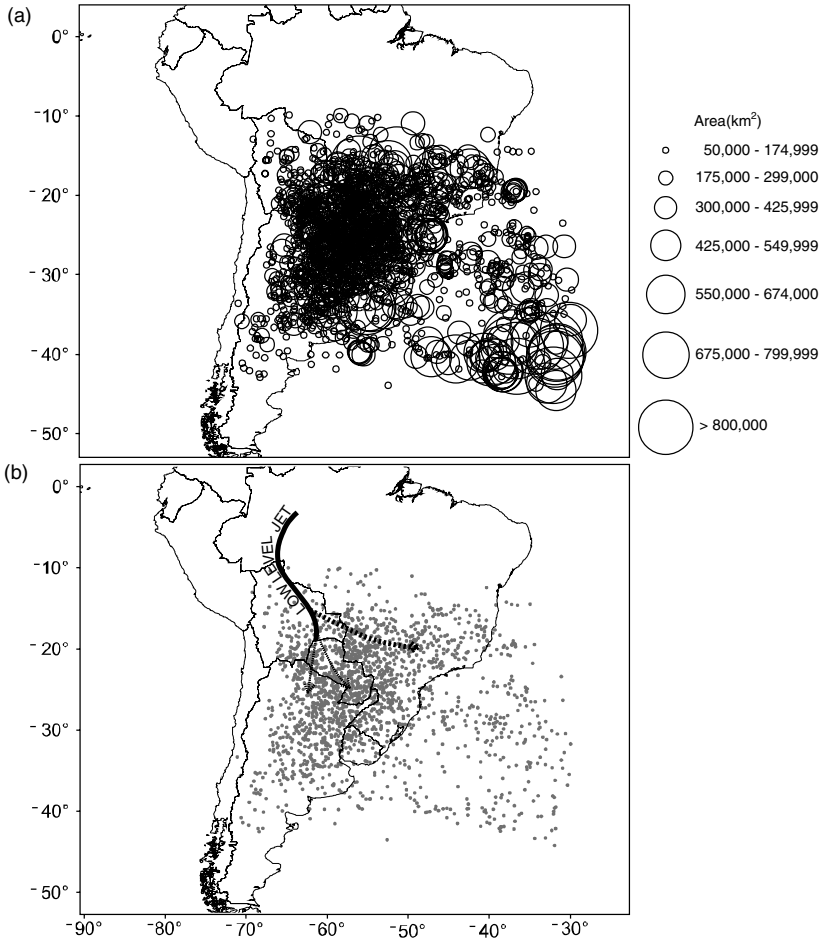

Figure 10. The locations of the (a) cloud shields and (b) a conceptual model of typical Amazonian low-level jet variability overlaid centroid locations from the 330 MCCs observed between the warm season months of October–May during 1998–2007.

DOI: 10.1002/joc

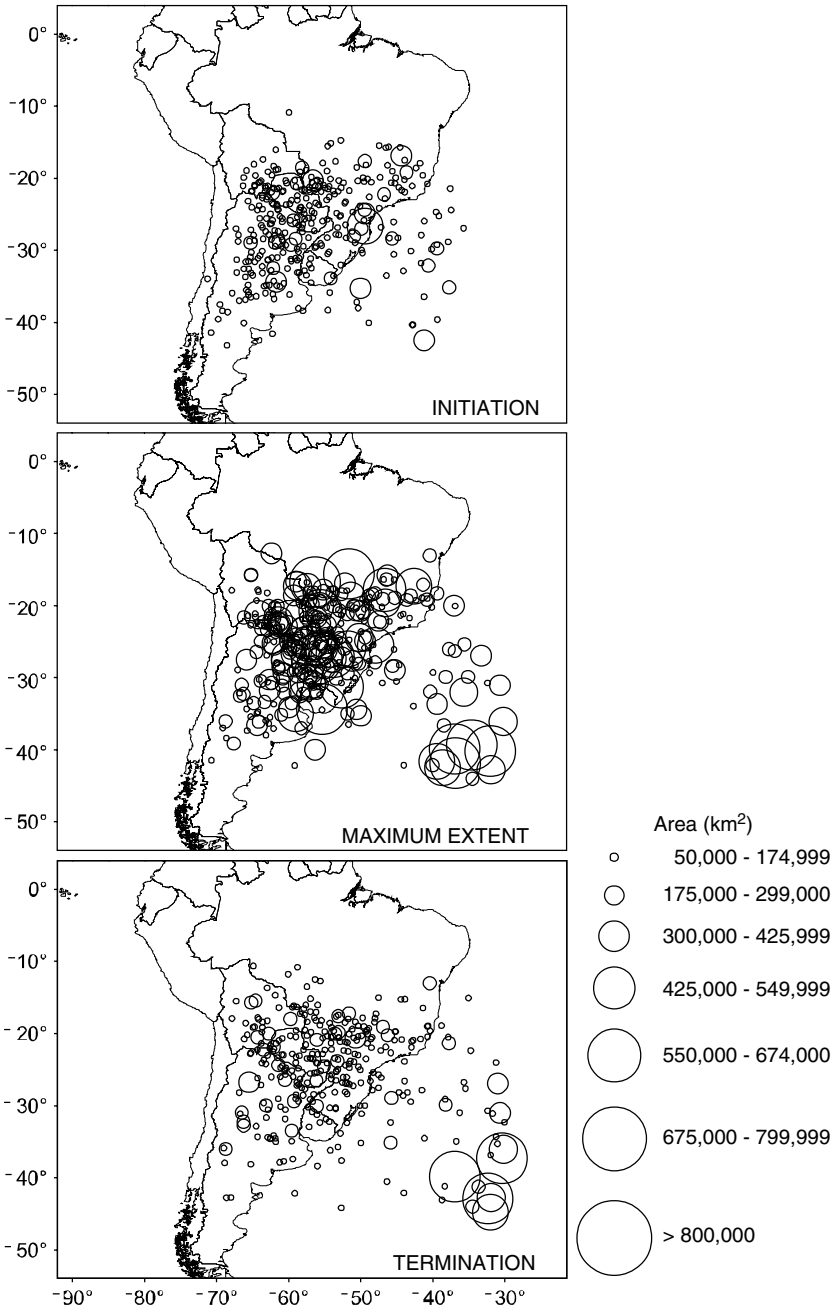

Figure 11. MCC cloud shields during critical stages observed between the warm season months of October–May during 1998–2007.

By examining the location of the cloud shields and cloud-shield centroids, one can see MCCs are most frequent over Paraguay, northern Argentina, and portions of southern Brazil (Figure 10). Organized convection and precipitation across tropical and subtropical continental areas of South America have been shown to be closely connected to locations near the exit region of the low-level jets (Saulo *et al*. 2007; Salio *et al*. 2007; Vera *et al*. 2006; Silva and Berbery 2006; Liebmann *et al*. 2004; Zipser *et al*. 2004; Nieto Ferreira *et al*. 2003; Marengo *et al*. 2002; Berbery and Collini 2000; Laing and Fritsch 2000; Nicolini and Saulo 2000; Velasco and Fritsch, 1987, among others). The same area also had the highest concentration of MCC cloud shields during each stage of their evolution (Figure 11). Specifically, MCCs were mostly located within the 20 °S–30 °S latitude band during all stages (Figure 12). These findings are especially important because the highest MCC precipitation rates are most likely to occur between storm initiation and maximum extent, while the greatest precipitation areas tend to occur near maximum extent (McAnelly and Cotton, 1989). In all warm seasons, the bulk of MCC activity was located between 20 °S and 30 °S (Figure 13), with the highest concentrations of MCCs over much of Paraguay and northern Argentina (Figure 14). The monthly analysis shows MCC frequency and concentration was greatest between 20 °S and 30 °S over Paraguay and northern Argentina

DOI: 10.1002/joc

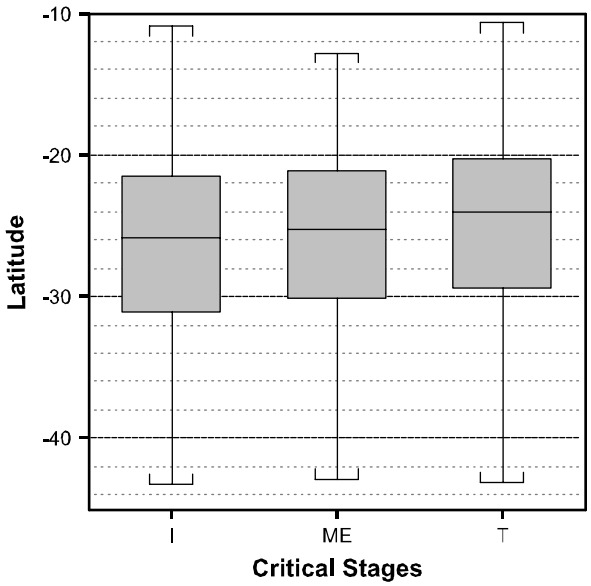

Figure 12. Box plots of the latitudinal distribution of MCC cloud-shield centroid locations during each stage, where 'I' is the initiation, 'ME' is the maximum extent, and 'T' is termination.

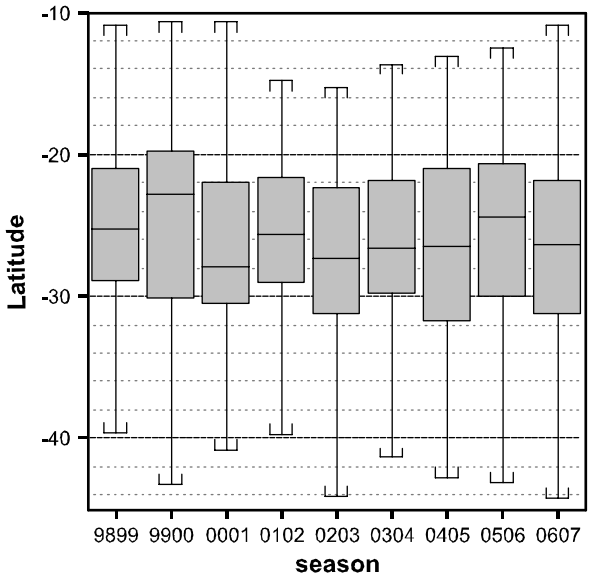

Figure 13. As in Figure 12 except by warm season.

during spring and summer. However, MCCs decreased in frequency and concentration, and exhibited a poleward shift in fall compared to summer (Figures 15 and 16).

In summary, VAF showed the preferred hub of MCC activity throughout the warm season over Paraguay and neighbouring areas of bordering countries. Results from this study lend support to that conclusion. From October through December, the frequency of MCCs increased at the same time they became more concentrated over Paraguay, northern Argentina, and portions of southern Brazil. In January, the frequency was similar to December, but MCCs became more widespread throughout the

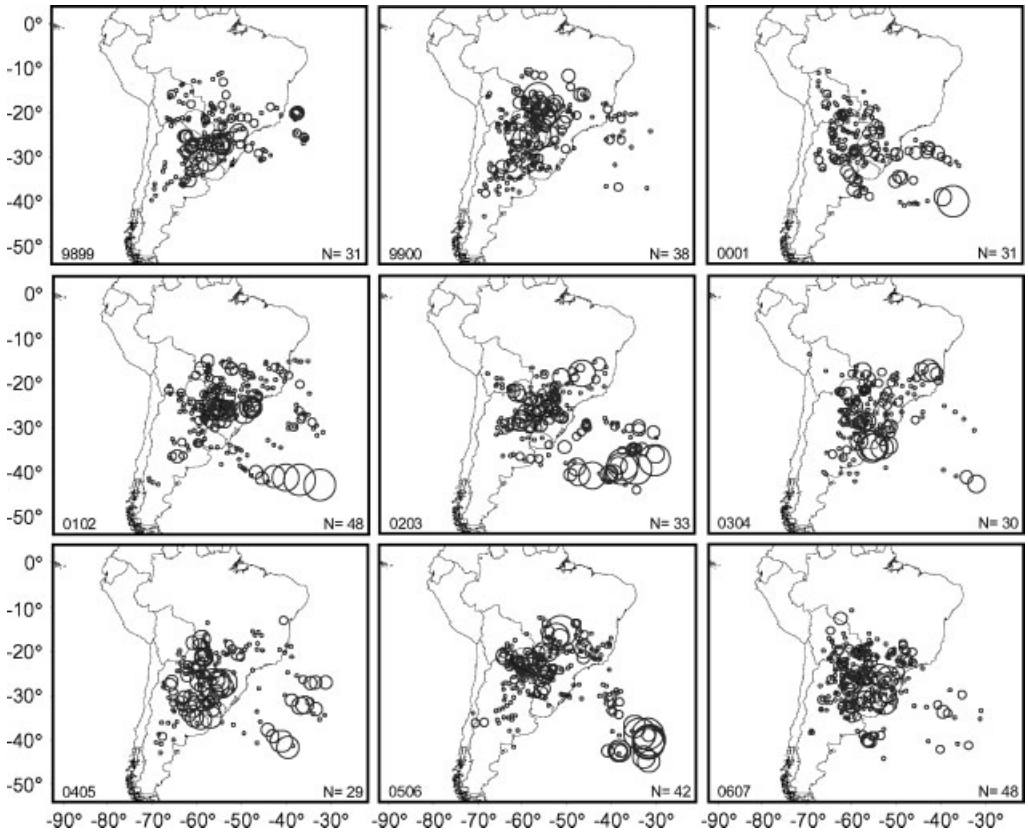

Figure 14. As in Figure 10 except by warm season. Note that *N* is equal to the number of MCC events during a given season and not the number of cloud shields.

DOI: 10.1002/joc

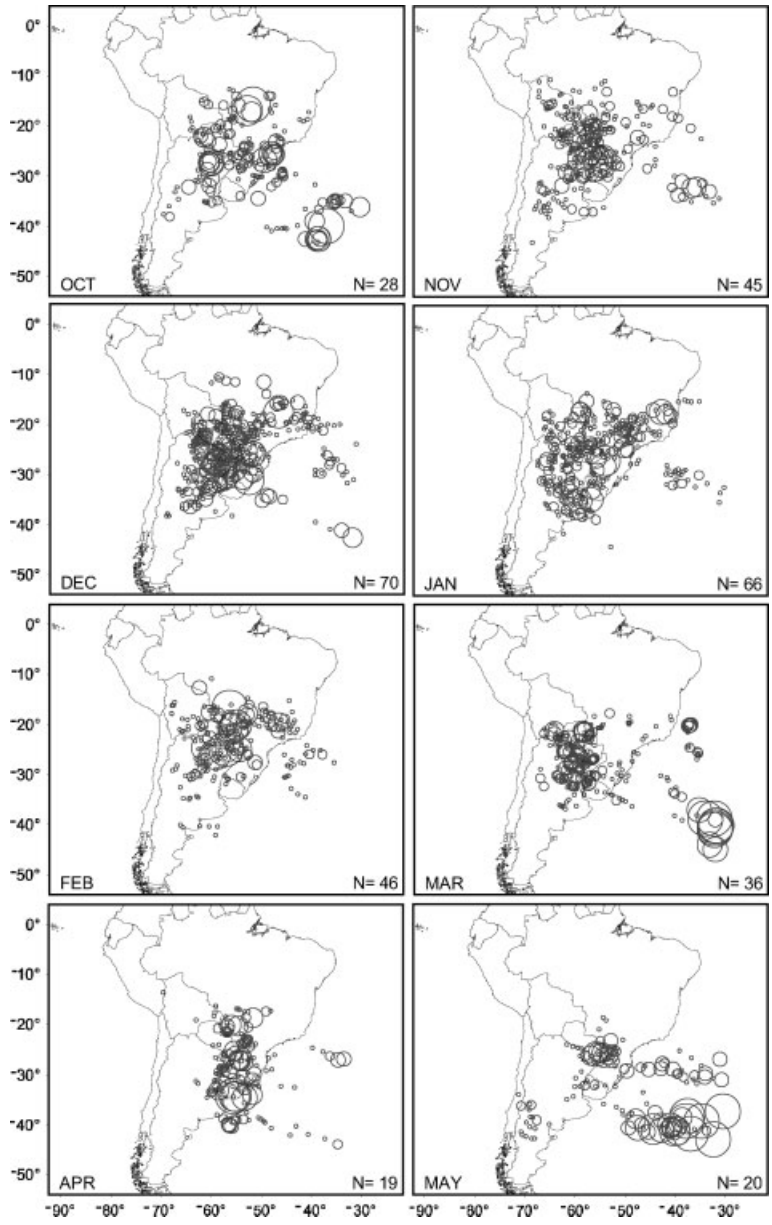

Figure 15. As in Figure 10 except by month.

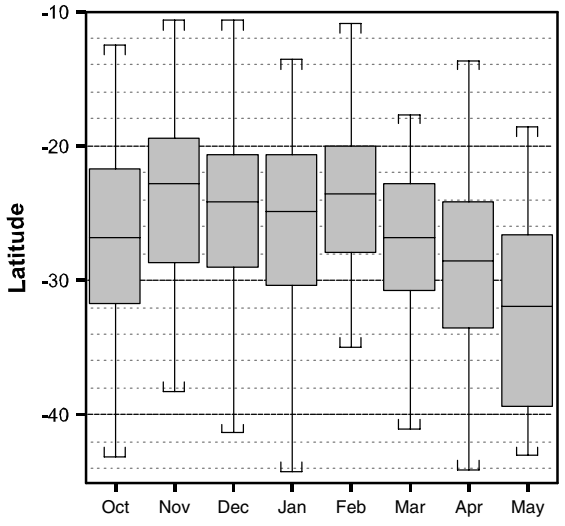

Figure 16. As in Figure 12 except by month.

region. Both the extent and frequency of MCCs diminished throughout the remainder of the warm season. However, from February to April a slight poleward shift in the highest concentration of MCCs occurred, which placed the maximum over northern Argentina. The primary difference between the final 2 months is that the cloud shields became less concentrated in May.

4.3. Comparison to previous work

One of the only available studies that documented MCCs across SSA prior to this work has been provided by VAF. The goal of this study was to extend their work and provide a more comprehensive analysis by examining the physical characteristics and spatial variability of MCCs across SSA for nine austral warm seasons during 1998–2007.

DOI: 10.1002/joc

Overall, the findings between the two studies are similar, but there are a few notable differences. The first difference is in the monthly frequency of MCCs. While our study shows a monthly frequency pattern closely resembling a normal distribution centred on a peak during December and January, VAF showed a distinct peak in November, nearly double the frequency found in any other month. Given that this study found that 80% of all MCCs occurred during November through March, we must conclude MCCs in SSA are tied to favourable synoptic environments (such as those described in Section 2).

Another difference between this work and VAF is MCC duration and maximum extent. Our results show MCCs in SSA have longer lifecycles than previously documented – a mean duration of 14 h (2.5 h longer than VAF). Our study also found MCCs reach an average maximum size of 256 500 km^2, or 27% larger than VAF. On the other hand, VAF used an 8°–12 °C colder cloud-top temperature threshold, which likely accounts for the smaller systems found in their study. Nevertheless, both studies highlight the fact that MCCs are very large, long-lasting, and frequently occurring events in SSA that possess great potential for contributing substantially to precipitation across the region.

4.4. Comparison between North and South American MCCs

This study utilized the 15-year US MCC database developed by Ashley *et al*. (2003) for a comparison of MCC characteristics between the American continents. As described in Section 2, North and South American MCCs share many similar physiographic and atmospheric environments. However, key differences in their environments may partially explain differences in the characteristics of North and South American MCCs. These are the clues that can enhance our understanding of these prolific rain-producing events.

It is important to note while Ashley *et al*. (2003) considered the entire year, comparisons made hereafter are based only on their warm season (April–August) statistics. Ashley *et al*. (2003) found an average warm-season frequency of 33 events in the USA, compared to the average 37 events for SSA. The lower US frequency might be explained by an examination of 8 months in this study compared to 5 months in Ashley *et al*. (2003). This study chose a longer period based on the relatively higher frequency of MCCs into the fall. VAF suggested the extended warm season in SSA may be accounted for by the influence of the oceans on the relatively smaller land mass. VAF also added that MCCs in SSA have a higher frequency at relatively lower latitudes compared the USA. Another difference exists within the monthly migratory patterns. Our study shows that MCC activity shows only a slight poleward migration towards the end of the warm season, whereas MCCs in the USA display distinct poleward displacement throughout each month. VAF suggested that these differences are likely explained by the migration pattern of the westerlies in both regions. The poleward shift in the westerlies is considerably greater over North America and MCC development tends to follow this pattern (VAF).

When comparing the differences between lifecycle durations and maximum sizes, the South American systems show remarkable differences from their North American counterparts. The maximum MCC cloud-shield size for the USA during the warm season is 164 600 km^2. An independent samples difference of means t-test was used to determine significant differences between North and South American MCC characteristics. Our results show MCCs in SSA are significantly larger, with an average size of 256 500 km^2 ($p = 0.01$). The results are similar for system durations. MCCs in SSA ($\overline{x} = 14$ h) last significantly longer than those of their North American counterpart ($\overline{x} = 10$ h) ($p = 0.01$).

Furthermore, Ashley *et al*. (2003) found MCCs had larger cloud shields and longer durations during the early warm season in the USA. As the warm season progresses, MCCs often develop smaller cloud shields with shorter durations. Ashley *et al*. (2003) suggested that these changes are tied to evolving synoptic and dynamic processes throughout the warm season. Tollerud and Rogers (1991) add that larger, longer-lived MCCs are more common during the early warm season due to proximities to moisture from the Gulf of Mexico. This study shows MCCs in SSA are somewhat larger and longer lasting during spring to early summer and fall compared to late summer systems. However, because a large proportion of MCC activity occurred between 20 °S and 30 °S, the relationship between latitude and MCC maximum extent or duration was weak ($p = 0.01$) (Figure 17). There was a significantly moderate relationship that showed longer-lived MCCs in SSA are often larger ($p = 0.01$) (Figure 18).

4.5. Continental *versus* Oceanic MCCs

While a large percentage of the global population of organized convective storms, including MCCs, are concentrated over continental regions (Zipser *et al*., 2006; Laing and Frisch, 1997), the subset of oceanic systems are worth comparing for a better understanding of organized thunderstorm activity. Furthermore, the global distribution of the relatively large cloud shields and often widely distributed rainfall associated with MCCs may even contribute substantially to global hydrologic and energy cycles (Laing *et al*., 1999; Velasco and Fritsch, 1987). Therefore, authors stratified the MCC climatology into oceanic and continental systems. Along the eastern coast of SSA, some MCCs would initiate over land and migrate over the ocean or vice versa. For these systems, an MCC was considered continental (oceanic) if two of the three critical storm stages occurred over the land (ocean).

The findings from the spatial analysis reveal that the majority of MCCs were located over South America, whereas a smaller population was found over the adjacent Atlantic Ocean. Specifically, out of the 330 MCCs

DOI: 10.1002/joc

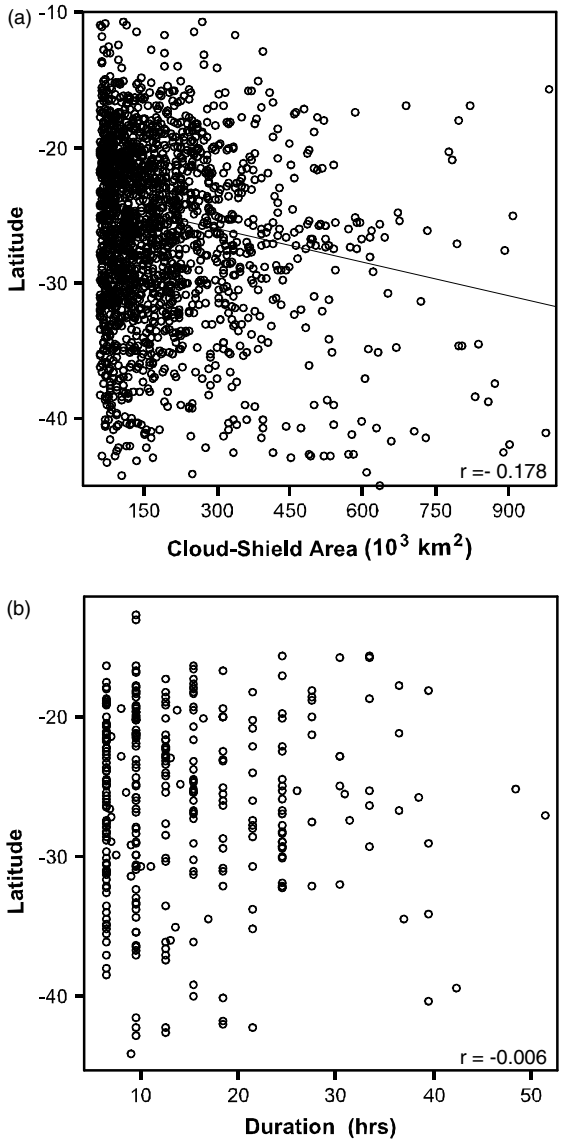

Figure 17. (a) Scatter plots showing relationships between latitude and cloud-shield area and (b) duration.

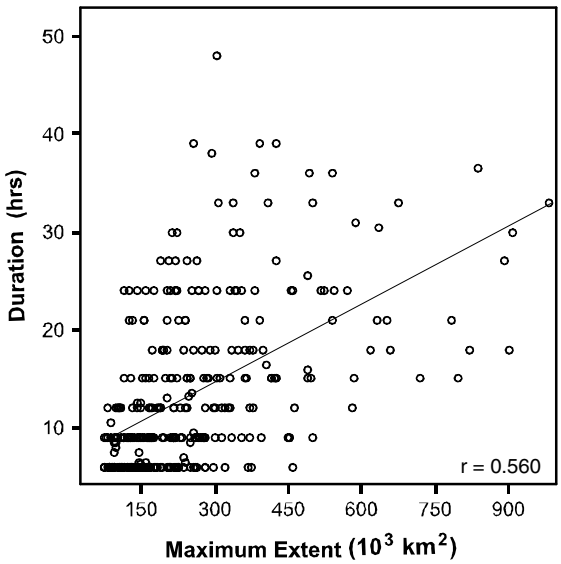

Figure 18. As in Figure 17 except for MCC maximum cloud-shield extent and duration.

observed during the study period, 85% were continental. Figure 19 shows that 83 and 75% of MCCs initiated over South America and the Atlantic Ocean between 1745 and 0245 UTC, respectively. Between 2045 and 0545 UTC 62% of MCCs reached maximum extent over the continent. While only 40% of oceanic MCCs reached maximum extent during the same time, 82% occurred between 1745 and 0845 UTC. Over South America and the Atlantic Ocean, 23 and 25% of MCCs dissipated at 0245 and 1445 UTC. In contrast to the findings of Nesbitt and Zipser (2003) that continental MCSs exhibit longer lifecycles, results from a Student's t-test show no significant differences between continental and oceanic MCC longevity. However, oceanic MCCs were significantly larger than continental systems at the time of maximum extent ($p = 0.01$), and for the entire lifecycle ($p = 0.01$)

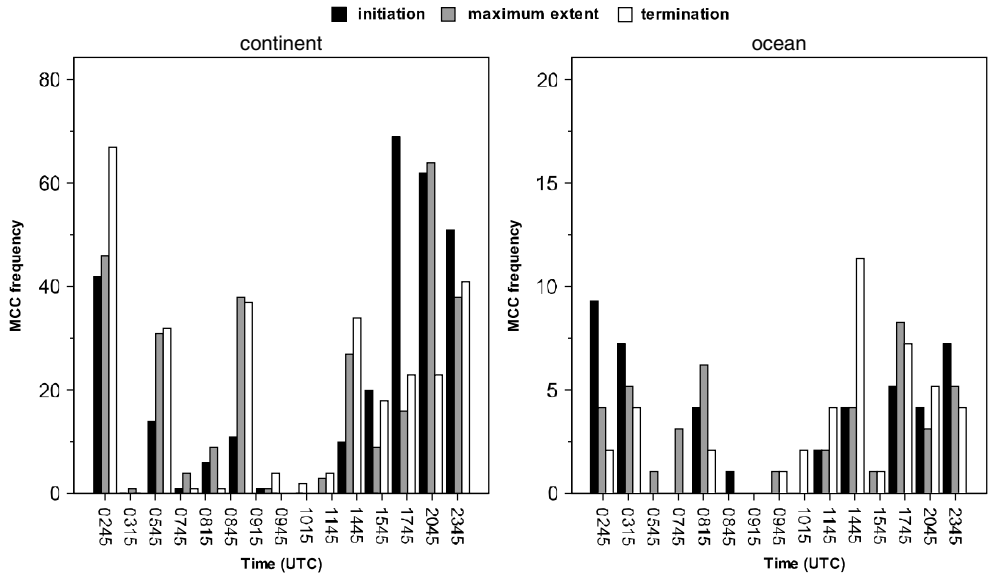

Figure 19. As in Figure 5 except for continental and oceanic MCCs.

DOI: 10.1002/joc

Table II. Mean size of continental and oceanic MCCs at the time of initiation (I), maximum extent (ME), and termination (T).

Cloud-shield size (km^2)	Continental			Oceanic		
	I	ME	T	I	ME	T
Critical stages	99 997	245 077*	104 187	115 889	332 558*	206 651
Overall		170 485*			241 378*	

* Significant difference of means between continental and oceanic systems (99% confidence interval).

(Table II). Furthermore, an examination of the intraseasonal relationship between MCC duration and maximum extent showed that only continental systems exhibited a significant relationship throughout the entire season ($p = 0.01$), with the strongest correlations throughout the warm season (Figure 20). In contrast, MCC maximum size and duration exhibited a significant relationship only late in the warm season ($p = 0.01$).

Laing and Fritsch (1997) indicated that characteristic differences and diurnal variability among various MCC population subsets (e.g. continental and oceanic systems) are likely driven by dynamic processes that are not directly connected to the diurnal radiation cycle. Such processes include diurnal circulation differences that are often related to land cover and topography (Laing and Frisch, 1997). Furthermore, gravity waves located just offshore have been shown to play an important role in the development and maintenance of thunderstorm activity (Mapes *et al*., 2003; Yang and Slingo, 2001; Silva Dias *et al*., 1987).

5. Conclusions

The subtropical region of South America is common place for intense thunderstorm activity. Over the recent

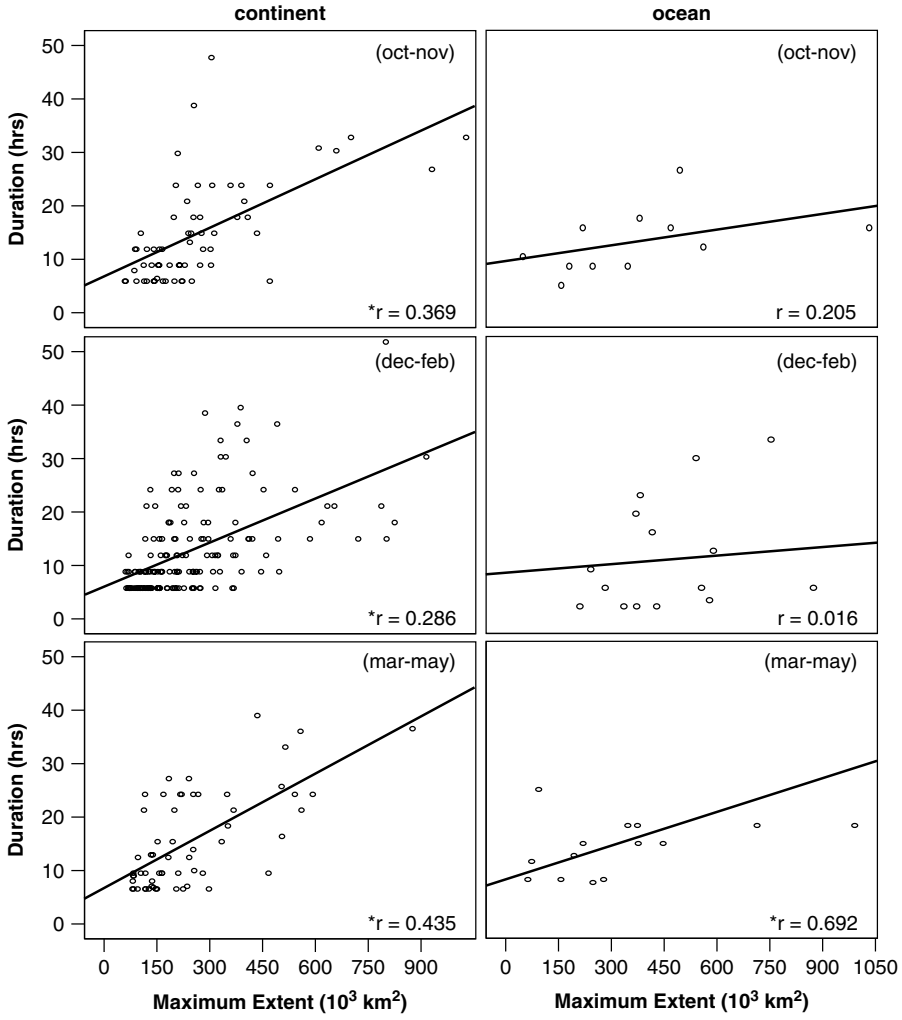

Figure 20. Scatter plots showing intraseasonal relationships between maximum cloud-shield extent and duration for continental and oceanic MCCs.

DOI: 10.1002/joc

decade, a great deal of research has been done to gain a better understanding of the convective events that occur there, and the physical environments that influence their behaviour. SSA is a region highly susceptible to heavy rainfall often produced from frequent occurrences of MCSs. This study extends the knowledge of South American MCS activity by focusing on the MCC, a particular subset of MCS that can produce prodigious precipitation.

This study used a hybrid automated/manual approach to identify and track 330 MCCs across SSA between October and May during 1998–2007. On average, there are 37 MCCs each warm season with peak frequencies during December and January. These are predominantly nocturnal events that largely take place east of the Andes between 20 °S and 30 °S. MCCs over SSA typically last 14 h and reach maximum sizes of 256 500 km^2. Due to the use of 3-hourly satellite data, some physical traits (e.g. lifecycle duration and maximum extent) are likely conservative estimates. Moreover, results from this work show considerable seasonal and monthly variability in the spatial distribution and physical characteristic of MCCs over SSA.

The monthly frequency and spatial distribution suggest MCCs over SSA are likely connected to certain synoptic and mesoscale processes favourable for their development. Specifically, peak MCC frequency and concentration patterns in Paraguay, northern Argentina, and southern Brazil during summer are indicative of minimum static stability common during this time of year. From the results found in VAF, Laing and Fritsch (2000) and Vera *et al*. (2006), steep lapse rates develop from ample low-level heat and moisture supply from the Amazon Basin, and cold-air advection from the high terrain of the upstream Andes. Upper-level disturbances rotate through a quasi-stationary subtropical jet-stream, which provide enhanced ascent for the onset of convection. The mean position of the subtropical jet relative to the areas of maximized low-level heat and moisture via the low-level jet helps explain the dominance of MCC activity between 20 °S and 30 °S. It is likely that other synoptic features that influence the low-level jet, including the South Atlantic Convergence Zone, may also play an important role in MCC behaviour and should be explored further.

Finally, a comparison between MCCs in the Americas shows that the systems in the Southern Hemisphere are significantly larger and longer-lasting events. A comparison between continental and oceanic systems shows that while the majority of MCCs are continental in origin, oceanic systems are significantly larger. Ashley *et al*. (2003) found that larger and longer-lasting MCCs also produce the greatest and most widespread rainfall. Few studies have examined MCS precipitation across SSA. However, the majority of the analyses of those studies are limited in scope to a few years or less. The effort should be made to provide a quantitative assessment of MCC rainfall in SSA. The dominant presence of MCC activity in Paraguay, northern Argentina, and southern Brazil suggests that these systems possess great potential for contributing substantially to precipitation totals across the region. The current study provides an excellent foundation for such a study.

Acknowledgements

The authors appreciate the assistance of Leila M. Vespoli de Carvalho (University of São Paulo) for her suggestions regarding MCC tracking, and the anonymous reviewers who provided insightful comments that helped to improve the manuscript.

References

Anderson CJ, Arritt RW. 1998. Mesoscale convective complexes and persistent elongated convective systems over the United States during 1992 and 1993. *Monthly Weather Review* **126**: 578–599.

Ashley WS, Mote TL, Dixon PG, Trotter SL, Durkee JD, Powell EJ, Grundstein AJ. 2003. Effects of mesoscale convective complex rainfall on the distribution of precipitation in the United States. *Monthly Weather Review* **131**: 3003–3017.

Augustine JA. 1985. *An Automated Method for the Documentation of Cloud-Top Characteristics of Mesoscale Convective Systems*. NOAA Tech. Memo. ERL ESG-10, NOAA/FSL, Boulder, CO, 121.

Berbery EH, Collini EA. 2000. Springtime and water vapor flux over southeastern South America. *Monthly Weather Review* **128**: 1328–1346.

Carvalho LMV, Jones C. 2001. A satellite method to identify structural properties of mesoscale convective systems based on maximum spatial correlation tracking technique (MASCOTTE). *Journal of Applied Meteorology* **40**: 1683–1701.

Carvalho LMV, Jones C, Liebmann B. 2002. Extreme precipitation events in southern South America and large-scale convective patterns in the South Atlantic Convergence Zone. *Journal of Climate* **15**: 2377–2394.

Cotton RW, McAnelly RL, Tremback CJ. 1989. A composite model of mesoscale convective complexes. *Monthly Weather Review* **117**: 765–783.

Duquia CG, Silva Dias MAF. 1994. Complexo convectivo de mesoescala: um estudo de caso para o oeste do Rio Grande do Sul. *VIII Congresso Brasileiro de Meteorologia, SBMET* **2**: 610–612.

Figueiredo JC, Scolar J. 1996. Estudo da trajetória dos sistemas convectivos de mesoescala na América do Sul. *VII Congresso Latino-Americano e Iberico de Meteorologia*, Buenos Aires, 165–166.

Fritsch JM, Kane RJ, Chelius CR. 1986. The contribution of mesoscale convective weather systems to the warm-season precipitation in the United States. *Journal of Applied Meteorology* **25**: 1333–1345.

Grimm AM, Barros VR, Doyle ME. 2000. Climate variability in southern South America associated with El Niño and La Niña events. *Journal of Climate* **13**: 35–58.

Grimm AM, Ferraz SET, Gomes J. 1998. Precipitation anomalies in Southern Brazil associated with El Niño and La Niña events. *Journal of Climate* **11**: 2863–2880.

Guedes RL. 1985. Condições de grande escala associadas a sistemas convectivos de mesoescala sobre a região central da América do Sul. Dissertação de Mestrado. IAG/USP, São Paulo, SP, 89.

Guedes RL, Silva Dias MAF. 1984. Estudo de tempestades severas associadas com o jato subtropical na América do Sul, *III Congresso Brasileiro de Meteorologia, SBMET*. Belo Horizonte, 3–7 Dezembro, 289–296.

Houze RA, Smull BF, Dodge P. 1990. Mesoscale organization of springtime rainstorms in Oklahoma. *Monthly Weather Review* **118**: 613–654.

Jackson JE. 1991. *A User's Guide to Principal Component Analysis*. Wiley-Interscience: New York; 569.

James J. 1992. A preliminary study of mesoscale convective complexes over the mid-latitudes of eastern Australia. Technical Report 66, Bureau of Meteorology: Melbourne, 30.

Kane RJ, Chelius CR, Fritsch JM. 1987. Precipitation characteristics of mesoscale convective weather systems. *Journal of Applied Meteorology* **26**: 1345–1357.

Laing AG, Fritsch JM. 1993a. Mesoscale convective complexes in Africa. *Monthly Wealther Review* **121**: 2254–2263.

DOI: 10.1002/joc

Laing AG, Fritsch JM. 1993b. Mesoscale convective complexes over the Indian monsoon region. *Journal of Climate* **6**: 911–919.

Laing AG, Fritsch JM. 1997. The global population of mesoscale convective complexes. *Quarterly Journal of the Royal Meteorological Society* **123**: 389–405.

Laing AG, Fritsch JM. 2000. The large-scale environments of the global populations of mesoscale convective complexes. *Monthly Weather Review* **128**: 2756–2776.

Laing AG, Fritsch JM, Negri AJ. 1999. Contribution of mesoscale convective complexes to rainfall in Sahelian Africa: estimates from geostationary infrared and passive microwave data. *Journal of Applied Meteorology* **38**: 957–964.

Lau KM, Zhou J. 2003. Anomalies of the South American summer monsoon associated with the 1997-99 El Niño-Southern Oscillation. *International Journal of Climatology* **23**: 529–539.

Liebmann B, Kiladis GN, Vera CS, Saulo AC, Carvalho LMV. 2004. Subseasonal variations of rainfall in South America in the vicinity of the low-level jet east of the Andes and comparison to those in the South Atlantic Convergence Zone. *Journal of Climate* **17**: 3829–3842.

Machado LAT, Rossow WB, Guedes RL, Walker AW. 1998. Life cycle variations of mesoscale convective systems over the Americas. *Monthly Weather Review* **126**: 1630–1654.

Maddox RA. 1979. A methodology for forecasting heavy convective precipitation and flash flooding. *National Weather Digest* **4**: 30–42.

Maddox RA. 1980. Mesoscale convective complexes. *Bulletin of the American Meteorological Society* **61**: 1374–1387.

Maddox RA. 1983. Large-scale meteorological conditions associated with mid-latitude mesoscale convective complexes. *Monthly Weather Review* **111**: 1475–1493.

Mapes BE, Warner TT, Xu MU. 2003. Diurnal patterns of rainfall in northwestern South America. Part III: diurnal gravity waves and nocturnal convection offshore. *Monthly Weather Review* **131**: 830–844.

Marengo JA, Douglas MW, Silva Dias PL. 2002. The South American low-level jet east of the Andes during the 1999 LBATRMM and LBA-WET AMC campaign. *Journal of Geophysical Research* **107**: 8079. DOI:10.1029/2001JD001188.

McAnelly RL, Cotton WR. 1989. The precipitation life cycle of mesoscale convective complexes over the central United States. *Monthly Weather Review* **117**: 784–808.

Mechoso RC, Días PS, Baetghen W, Barros V, Berbery EH, Clarke R, Cullen H, Ereño C, Grassi B, Lettenmaier D. 2001. *Climatology and Hydrology of the La Plata Basin*. Document of VAMOS/CLIVAR document. 56. Available online: http://www.clivar.org/organization/vamos/index.htm.

Merritt JH, Fritsch JM. AMS. 1984. On the movement of the heavy precipitation areas of mid-latitude mesoscale convective complexes. Preprints, *10 th Conference Weather Forecasting and Analysis*, Tampa, FL, 529, 536.

Miller D, Fritsch JM. 1991. Mesoscale convective complexes in the western Pacific region. *Monthly Weather Review* **119**: 2978–2992.

Mota GV. 2003. Characteristics of rainfall and precipitation features defined by the Tropical Rainfall Measuring Mission over South America. Ph.D. dissertation, University of Utah, 215.

National Oceanic Atmospheric Administration (NOAA). *The Comprehensive Large Array-data Stewardship System* (CLASS). 2007. Silver Spring, MD. Available online: http://www.class.noaa.gov.

Nesbitt SW, Zipser EJ. 2003. The diurnal cycle of rainfall and convective intensity according to three years of TRMM measurements. *Journal of Climate* **16**: 1456–1475.

Nicolini M, Saulo AC. American Meteorological Society. 2000. ETA characterization of the 1997–98 warm season Chaco jet cases. Preprints *Sixth International Conference on Southern Hemisphere Meteorology and Oceanography*, Santiago, Chile, 330–331.

Nieto Ferreira RN, Rickenbach TM, Herdies DL, Carvalho LMV. 2003. Variability of South American convective cloud systems and tropospheric circulation during January–March 1998 and 1999. *Monthly Weather Review* **131**: 961–973.

Rocha RP. IAG/USP. 1992. Simulação numérica de sistema de mesoescala sobre a América do Sul. Dissertação de Mestrado. University of São Paulo, São Paulo.

Rodgers DM, Howard KW, Johnston EC. 1983. Mesoscale convective complexes over the United States during 1982. *Monthly Weather Review* **111**: 2363–2369.

Ropelewski CF, Halpert MS. 1987. Global and regional scale precipitation patterns associated with the El Niño/Southern Oscillation. *Monthly Weather Review* **115**: 1606–1625.

Ropelewski CF, Halpert MS. 1989. Precipitation patterns associated with the high-index phase of the Southern Oscillation. *Journal of Climate* **2**: 268–284.

Salio P, Nicolini M, Zipser EJ. 2007. Mesoscale convective systems over southeastern South America and their relationship with the South American low-level jet. *Monthly Weather Review* **135**: 1290–1309.

Saulo C, Ruiz J, Skabar YG. 2007. Synergism between the low-level jet and organized convection at its exit region. *Monthly Weather Review* **135**: 1310–1326.

Scolar J, Figueiredo JC. 1990. Análise das condições sinóticas associadas à formação de Complexos Convectivos de Mesoescala. *VI Congresso Brasileiro de Meteorologia* SBMET Anais, 2, 457–461.

Silva VBS, Ambrizzi T. 2006. Inter-El Niño variability and its impact on the South American low-level jet east of the Andes during austral summer – two case studies. *Advances in Geosciences* **6**: 283–287.

Silva VBS, Berbery EH. 2006. Intense rainfall events affecting the La Plata Basin. *Journal of Hydrometeorology* **7**: 769–787.

Silva Dias PL, Bonatti JP, Kousky VE. 1987. Diurnally forced tropical tropospheric circulation over South America. *Monthly Weather Review* **115**: 1465–1478.

Tollerud EI, Collander RS. International Association of Hydrological Sciences. 1993. Mesoscale convective systems and extreme rainfall in the central United States. Extreme hydrological events: precipitation,floods and droughts. *Hydrological Science* **213**: 11–19.

Tollerud EI, Rodgers DM. 1991. The seasonal and diurnal cycle of mesoscale convection and precipitation in the central United States: Interpreting a 10-year satellite-based climatology of mesoscale convective complexes. Preprints, *7th Conference on Applied Meteorology*. Salt Lake City.

Tollerud EI, Rodgers DM, Brown K. 1987. Seasonal, diurnal, and geographic variations in the characteristics of heavy-rain-producing mesoscale convective complexes: a synthesis of eight years of MCC summaries. Preprints, *11thConference Weather Modification*. Edmonton, 143–146.

Velasco I, Fritsch JM. 1987. Mesoscale convective complexes in the Americas. *Journal of Geophysical Research Letters* **92**: 9591–9613.

Vera C, Baez J, Douglas M, Manuel CB, Marengo J, Meitin J, Nicolini M, Nogues-Paegle J, Paegle J, Penalba O, Salio P, Silva Dias MA, Silva Dias P, Zipser EJ. 2006. The South American low-level jet experiment. *Bulletin of the American Meteorological Society* **87**: 63–77.

Yang G-Y, Slingo J. 2001. The diurnal cycle in the Tropics. *Monthly Weather Review* **129**: 784–801.

Zipser EJ, Cecil DJ, Liu C, Nesbitt SW, Yorty DP. 2006. Where are the most intense thunderstorms on Earth? *Bulletin of the American Meteorological Society* **87**: 1057–1071.

Zipser EJ, Salio P, Nicolini M. 2004. Mesoscale convective systems activity during SALLJEX and the relationship with SALLJ. *CLIVAR Exchanges*,No. 9, International CLIVAR Project Office, Southampton, United Kingdom, 14–16.

DOI: 10.1002/joc